Neuropsychopharmacology (2017) 42, 2504–2515
© 2017 American College of Neuropsychopharmacology. All rights reserved 0893-133X/17
www.neuropsychopharmacology.org

Intranasal Lactoferrin Enhances α-Secretase-Dependent Amyloid Precursor Protein Processing via the ERK1/2-CREB and HIF-1α Pathways in an Alzheimer's Disease Mouse Model

Chuang Guo*[,1], Zhao-Hui Yang[1,2], Shuai Zhang[1,2], Rui Chai[1], Han Xue[1], Yan-Hui Zhang[1], Jia-Yi Li[1] and Zhan-You Wang*[,1]

[1]*Institute of Neuroscience, College of Life and Health Sciences, Northeastern University, Shenyang, China*

Growing evidence suggests that lactoferrin (Lf), an iron-binding glycoprotein, is a pleiotropic functional nutrient. In addition, Lf was recently implicated as a neuroprotective agent. These properties make Lf a valuable therapeutic candidate for the treatment of Alzheimer's disease (AD). However, the mechanisms regulating the physiological roles of Lf in the pathologic condition of AD remain unknown. In the present study, an APPswe/PS1DE9 transgenic mouse model of AD was used. We explored whether intranasal human Lf (hLf) administration could reduce β-amyloid (Aβ) deposition and ameliorate cognitive decline in this AD model. We found that hLf promoted the non-amyloidogenic metabolism of amyloid precursor protein (APP) processing through activation of α-secretase a-disintegrin and metalloprotease10 (ADAM10), resulting in enhanced cleavage of the α-COOH-terminal fragment of APP and the corresponding elevation of the NH2-terminal APP product, soluble APP-α (sAPPα), which consequently reduced Aβ generation and improved spatial cognitive learning ability in AD mice. To gain insight into the molecular mechanism by which Lf modulates APP processing, we evaluated the involvement of the critical molecules for APP cleavage and the signaling pathways in N2a cells stably transfected with Swedish mutant human APP (APPsw N2a cells). The results show that the ERK1/2-CREB and HIF-1α signaling pathways were activated by hLf treatment, which is responsible for the expression of induced ADAM10. Additional tests were performed before suggesting the potential use of hLf as an antioxidant and anti-inflammatory. These findings provide new insights into the sources and mechanisms by which hLf inhibits the cognitive decline that occurs in AD via activation of ADAM10 expression in an ERK1/2-CREB and HIF-1α-dependent manner.
Neuropsychopharmacology (2017) **42,** 2504–2515; doi:10.1038/npp.2017.8; published online 26 April 2017

INTRODUCTION

Lactoferrin (Lf), an iron-binding glycoprotein produced in exocrine secretions such as milk, saliva, and tears and in neutrophilic leukocytes (Johnson and Wessling-Resnick, 2012), is thought to play an important role in iron metabolism (Aisen and Leibman, 1972); to have anti-inflammatory, immunomodulator, antioxidant, and anticarcinogenic properties; to play a role in the host defense mechanism; and to serve as a growth factor (Garcia-Montoya *et al*, 2012; Orsi, 2004). Of particular note, several observations have strongly suggested that Lf is expressed in many neurons and in some astrocytes, microglia, and oligodendrocytes of the human brain (Arnold *et al*, 1977; Kawamata *et al*, 1993) and that it could participate in aging processes and Alzheimer's disease (AD) progression (Kawamata *et al*, 1993; Leveugle *et al*, 1994; Qian and Wang, 1998). Previous studies have shown that Lf is highly expressed in both extracellular senile plaques composed of aggregated *β*-amyloid (A*β*) peptide and in intracellular neurofibrillary tangles composed of aggregated hyperphosphorylated tau protein, which are the two major neuropathological hallmarks of AD in the brains of human AD specimens and amyloid precursor protein (APP) transgenic (Tg) mice, suggesting the link of Lf and AD-like pathologies (Kawamata *et al*, 1993; Selkoe, 1989; Wang *et al*, 2010). However, the reason for the upregulation of Lf in the brains of both AD patients and Tg AD mice has been poorly documented so far. Due to its well-described anti-inflammatory and antioxidant abilities, we inferred that Lf may exert a protective effect against AD (Rousseau *et al*, 2013; Wang *et al*, 2010). Recently, studies have suggested that the internalized exogenous Lf by lactoferrin receptor (LfR) play neuroprotective role on the ventral mesencephalon neurons against MPP^+ *in vitro* (Wang *et al*, 2015) can also protect the preterm brain against hypoxia-ischemia injury and revert some of the intrauterine growth restriction-induced brain hippocampal changes *in vivo* (van de Looij *et al*, 2014). An interesting study showed that intraperitoneal injection of deferasirox-Lf conjugates was able to significantly attenuate learning deficits

*Correspondence: Dr C Guo or Professor Z-Y Wang, College of Life and Health Sciences, Northeastern University, Shenyang 110819, China, Tel/Fax: +86 24 22529997, E-mail: guoc@mail.neu.edu.cn or wangzy@mail.neu.edu.cn
[2]These two authors contributed equally to this work.
Received 22 August 2016; revised 3 January 2017; accepted 7 January 2017; accepted article preview online 12 January 2017

induced by Aβ injection in a rat model of AD through metal chelation therapy (Kamalinia *et al*, 2013). The iron chelator deferoxame (DFO) has been shown to provide neuroprotective effects in clinical patients and animal models of AD (Crapper McLachlan *et al*, 1991; Guo *et al*, 2013), for which the mechanism may be regulation of the transcriptional activator hypoxia-inducible factor 1α (HIF-1α) (Guo *et al*, 2015). Lf exhibits similar chelating features as DFO (Kontoghiorghes *et al*, 2010; Kruzel *et al*, 2010) and functions as a normoxic mimetic of hypoxia capable of stabilizing HIF-1α (Zakharova *et al*, 2012). It is important to consider that Lf prevents some denatured/misfolded proteins from aggregating (Takase, 1998), and its multifunctional anti-prion activities have been identified (Iwamaru *et al*, 2008). These properties make Lf a valuable therapeutic candidate against AD. However, until now, no detailed studies dedicated to the links between the chelating properties of Lf and its protective features, especially with respect to the ability of Lf to directly control Aβ production and, in particular, APP metabolism in AD, have been reported. Thus, it is of utmost importance to document whether Lf can interfere with APP processing through the regulation of APP-cleaving secretases. In this context, we have shown that DFO can reverse iron-induced memory deficits through inhibiting amyloidogenic APP processing in APP/PS1 double Tg mice (Guo *et al*, 2013).

Aβ peptides, products of amyloidogenic APP processing, and plaques are known to play central roles in the neuropathology of AD (Abbott, 2008). Alternatively, APP can be processed by a-disintegrin and metalloproteinase 10 (ADAM10) pathway that prevents the formation of toxic Aβ and gives rise to the secretion of soluble α-secretase-released N-terminal APP domains (sAPPα) and α-COOH-terminal fragments (α-CTF) (Lammich *et al*, 1999; Vincent and Govitrapong, 2011). The sAPPα fragment has been shown to have both neuroprotective and neurotrophic capabilities, suggesting that the presence of sAPPα in the milieu interne may improve neuronal viability (Mattson *et al*, 1993; Turner *et al*, 2003). Thus, various synthetic and naturally occurring compounds have been studied to determine their therapeutic potential for promoting non-amyloidogenic processing of APP (Shukla *et al*, 2015; Vardy *et al*, 2005). These data strongly support the hypothesis that Lf could behave as a positive regulator of the non-amyloidogenic/α-secretase pathway.

This study investigates the capability of Lf to stimulate the non-amyloidogenic processing of APP and α-secretase catalytic activity and expression in APP/PS1 mice. We also address the molecular mechanisms by which Lf alters APP processing. Specifically, Lf enhanced the expression of ADAM10 via an ERK-CREB- and HIF-1α-dependent mechanism to protect mice against cognitive deficits. These findings suggest a novel neuroprotective role for Lf-mediated APP processing in neurodegenerative disorders, including AD.

MATERIALS AND METHODS

Transgenic Mice and Treatments

The male APP/PS1 mice used in this research were originally obtained from the Jackson Laboratory (West Grove, PA). The mice were raised in a controlled environment (22–25 °C room temperature, 40–60% relative humidity, and 12 h light/dark cycle) with free access to food and water. The Laboratory Animals Ethical Committee of Northeastern University approved all experimental procedures.

Mice at the age of 6 months were randomly divided into one of three treatment groups (eight mice per group): vehicle control, 2 mg/kg human Lf (hLf; Sigma-Aldrich, L4040), and 6 mg/kg hLf. hLf dissolved in saline was administered by intranasal delivery once a day for 3 months, and vehicle control mice were given saline. The dosages of hLf were chosen based on a previous report (Velusamy *et al*, 2014). Body weight and general health of the mice were observed daily.

Morris Water Maze Test

Spatial learning and memory were tested using the Morris water maze as described in our previous studies (Guo *et al*, 2013). For spatial learning, the mice were trained in the water maze to find a visible platform for 2 consecutive days with four trials per day. On each trial, the mouse was given 60 s to climb onto the platform. Then, the place navigation test with a hidden platform was performed for four trials per day with a 1-min interval between trials for 5 consecutive days. The swimming path and the time used to find the platform (latency) were recorded. For spatial memory, the platform was removed after training. A 1-min probe trail was tested for 2 days. The number of times that each mouse crossed the target platform quadrant was recorded. Finally, the recorded data were statistically analyzed.

Tissue Preparation

At the conclusion of behavioral testing (at 9.5 months of age), mice were killed under sodium pentobarbital (50 mg/kg, intraperitoneally) anesthesia. The brains were immediately removed and dissected in half on an ice-cold board. One-half of the brain was postfixed in 4% paraformaldehyde solution and embedded in paraffin for morphological assessment. The other half was frozen at −80 °C for biochemical analyses.

Cell Culture

Mouse neuroblastoma 2a (N2a) cells stably transfected with Swedish mutant human APP (APPsw N2a cells) were kindly provided by Dr Huaxi Xu at the Burnham Institute. The cells were grown in media containing 50% Dulbecco's modified Eagle's medium (DMEM; Gibco, Carlsbad, CA) supplemented with 50% Opti-MEM, 100 U/ml penicillin, 100 µg/ml streptomycin, 200 µg/ml G418 (GIBCO/Invitrogen, Burlington, ON), and 10% fetal bovine serum (FBS) (Gibco) in a humidified air atmosphere with 5% CO_2 at 37 °C. To determine whether Lf could affect the activities of α-secretases in the cells, the cells were grown in serum-free medium for an additional 24 h before incubation with inhibitors in the absence or presence of 0.1 mg/ml hLf (Sigma-Aldrich, L4894), as previously described (Wang *et al*, 2015). Thereafter, the medium was removed, and the cells were harvested for Western blot analysis.

Immunohistochemistry and Immunofluorescence

Coronal paraffin sections (5 μm) were dewaxed and rehydrated, and antigen retrieval was achieved by boiling in citric acid buffer for 3 min in a microwave oven. The sections were then incubated overnight with mouse anti-Aβ (1 : 500; Sigma) at 4 °C. After rinsing, sections were incubated with anti-mouse IgG (1 : 200), conjugated with horseradish peroxidase (HRP), and detected with 0.025% DAB, as previously described (Guo *et al*, 2013). APPsw N2a cells were fixed with 4% paraformaldehyde at room temperature for 30 min after the indicated treatment periods. After rinsing, treatment with normal donkey serum (Jackson ImmunoResearch Laboratory, West Grove, PA, USA) for 1 h at room temperature was used to block non-specific binding. For double immunofluorescence, tissue sections (10 μm) or cell cultures were incubated with mouse anti-Aβ (1 : 500; Sigma) and rabbit anti-glial fibrillary acidic protein (GFAP, 1 : 100; Santa Cruz Biotechnology), mouse anti-Aβ (1 : 500; Sigma) and rabbit anti-ionized calcium-binding adaptor molecule 1 (Iba1, 1 : 100; Abcam), mouse anti-Aβ (1 : 500; Sigma) and rabbit anti-synaptophysin (SYP, 1 : 200; Abcam), mouse anti-Aβ (1 : 500; Sigma) and rabbit anti-HIF-1α (1 : 200; Cell Signaling Tech(CST)), and mouse anti-Aβ

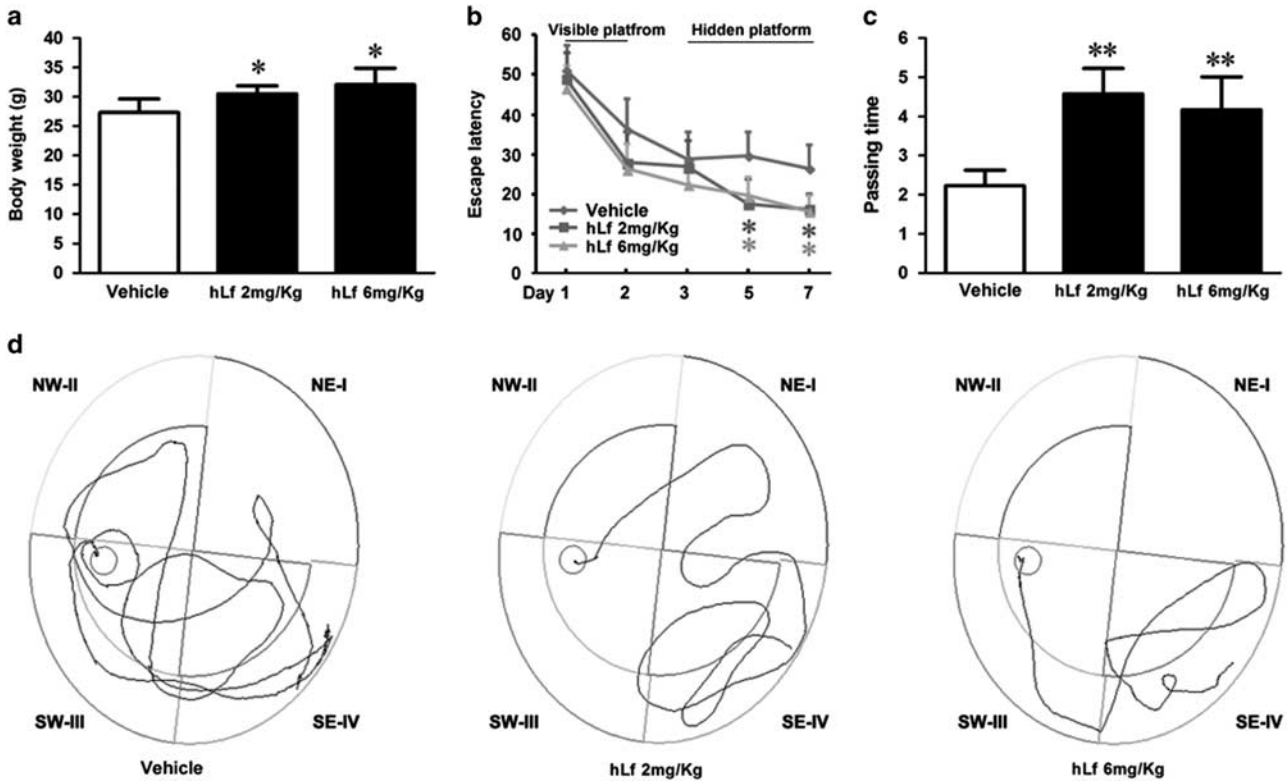

Figure 1 Lactoferrin (Lf) treatment increases body weight gain and rescues cognitive decline in amyloid precursor protein (APP)/presenilin 1 (PS1) mice. APP/PS1 transgenic (Tg) mice at the age of 6 months were treated with human Lf (hLf) (2 mg/kg per day or 6 mg/kg day) for 3 months before their body weights and cognitive abilities were evaluated. (a) The body weights of the mice were increased in the hLf-treated group relative to vehicle controls. (b) During MWM training from day 1 to day 2, the results of the visible platform tests did not differ among the groups, whereas the hLf-treated APP/PS1 mice showed a decrease in escape latency from the fifth day to the seventh day of testing in the hidden platform tests. (c) In the probe trial toward the target quadrant on the eighth day, the passing times of the mice in the hLf treatment group were significantly increased compared with the mice in the untreated group. (d) The motion tracking of the mice in the different groups is shown for the hidden platform tests. All values are the means ± SEM ($n = 8$). *$p < 0.05$, **$p < 0.01$ compared with the vehicle group.

Figure 2 Lactoferrin (Lf) treatment reduced β-amyloid (Aβ) plaque accumulation and synapse loss in amyloid precursor protein (APP)/presenilin 1 (PS1) mouse brains. (a) Immunohistochemical staining investigating the distribution of Aβ plaques in the cortex and hippocampus of the APP/PS1 mouse brains. (b) Western blot analysis demonstrated that the synaptophysin (SYP) protein levels were markedly increased in the human Lf (hLf)-treated mouse brains compared with the vehicle-treated mouse brains. β-actin was used as an internal control. (c) Immunofluorescence labeling and confocal microscopy analysis revealed the distribution and expression of anti-SYP (red) and Aβ (green) in the brain sections of the APP/PS1 mice. Scale bar = 100 μm. (d) Western blot analysis showed the levels of APP cleavage enzymes and products. β-actin was used as an internal control. (e) hLf treatment resulted in significantly decreased levels of APP. (f–h) hLf treatment significantly increased the levels of ADAM10 and PS1, whereas there were no significant changes in the BACE1 levels in the brain tissues between the vehicle- and hLf-treated mice. (i–l) hLf led to an augmentation of sAPPα secretion with a concomitant increase in C83. There were no significant differences in the levels of sAPPβ and C99 in the hLf-treated mice compared with vehicle controls. All values are the means ± SEM ($n = 8$). *$p < 0.05$, **$p < 0.01$ compared with the vehicle group. A full color version of this figure is available at the *Neuropsychopharmacology* journal online.

(1 : 500; Sigma) and rabbit anti-ADAM10 (1 : 100; CST) primary antibodies overnight at 4 °C. The immunoreactivity was subsequently determined using donkey anti-mouse IgG conjugated with fluorescein isothiocyanate (1 : 200; Jackson ImmunoResearch Laboratories) and Texas-Red donkey anti-rabbit IgG (1 : 200; Jackson ImmunoResearch Laboratories)

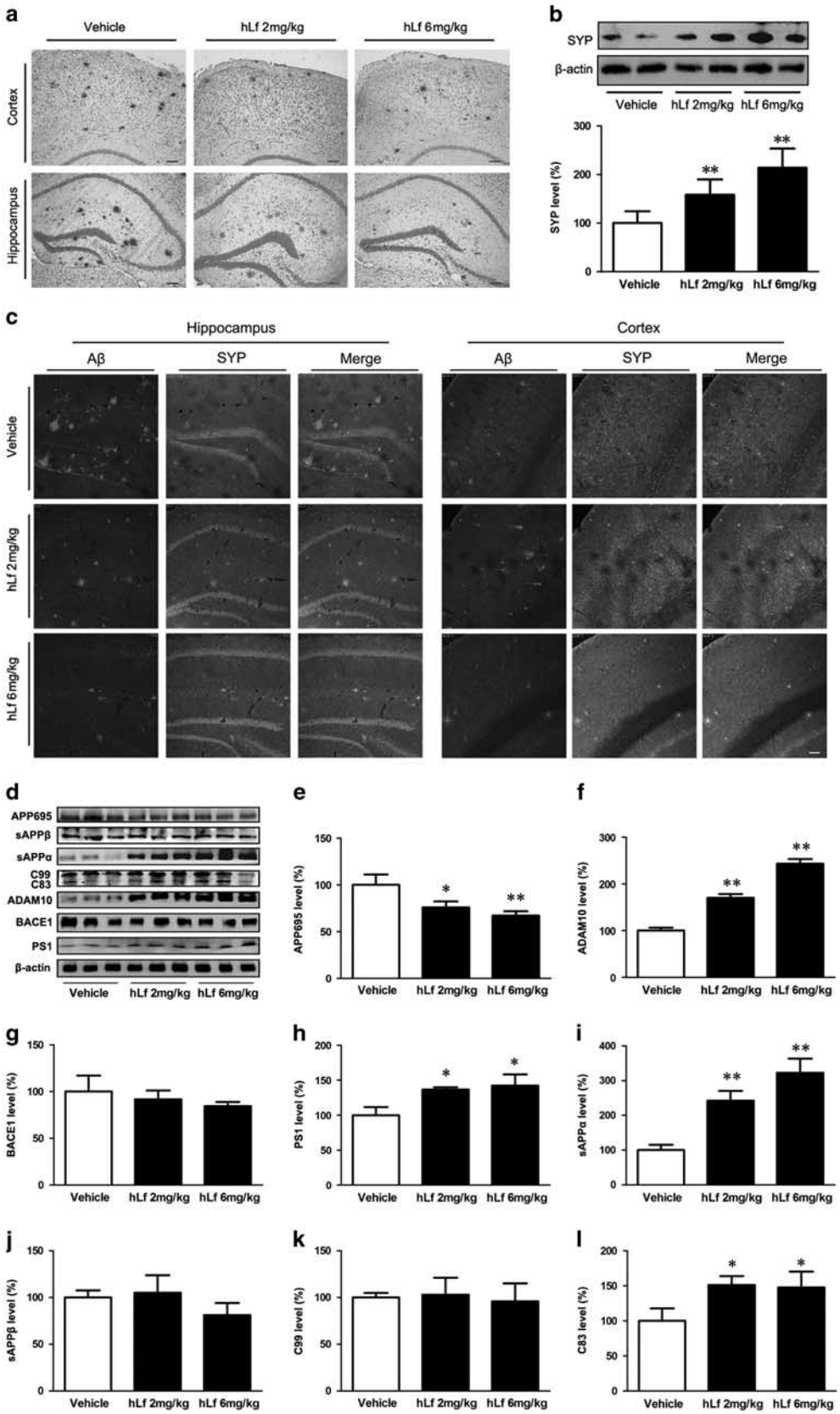

secondary antibodies for 2 h at room temperature followed by staining with DAPI for 5 min. The images were observed using a confocal laser scanning microscope (SP8, Leica). No fluorescence is expected when the primary antibody is omitted.

Western Blotting

The tissue samples were lysed in a sample buffer (150 mM NaCl, 1% Nonidet P-40, 0.5% deoxycholic acid, 0.1% sodium dodecyl sulfate (SDS), and 50 mM Tris, pH 8.0)

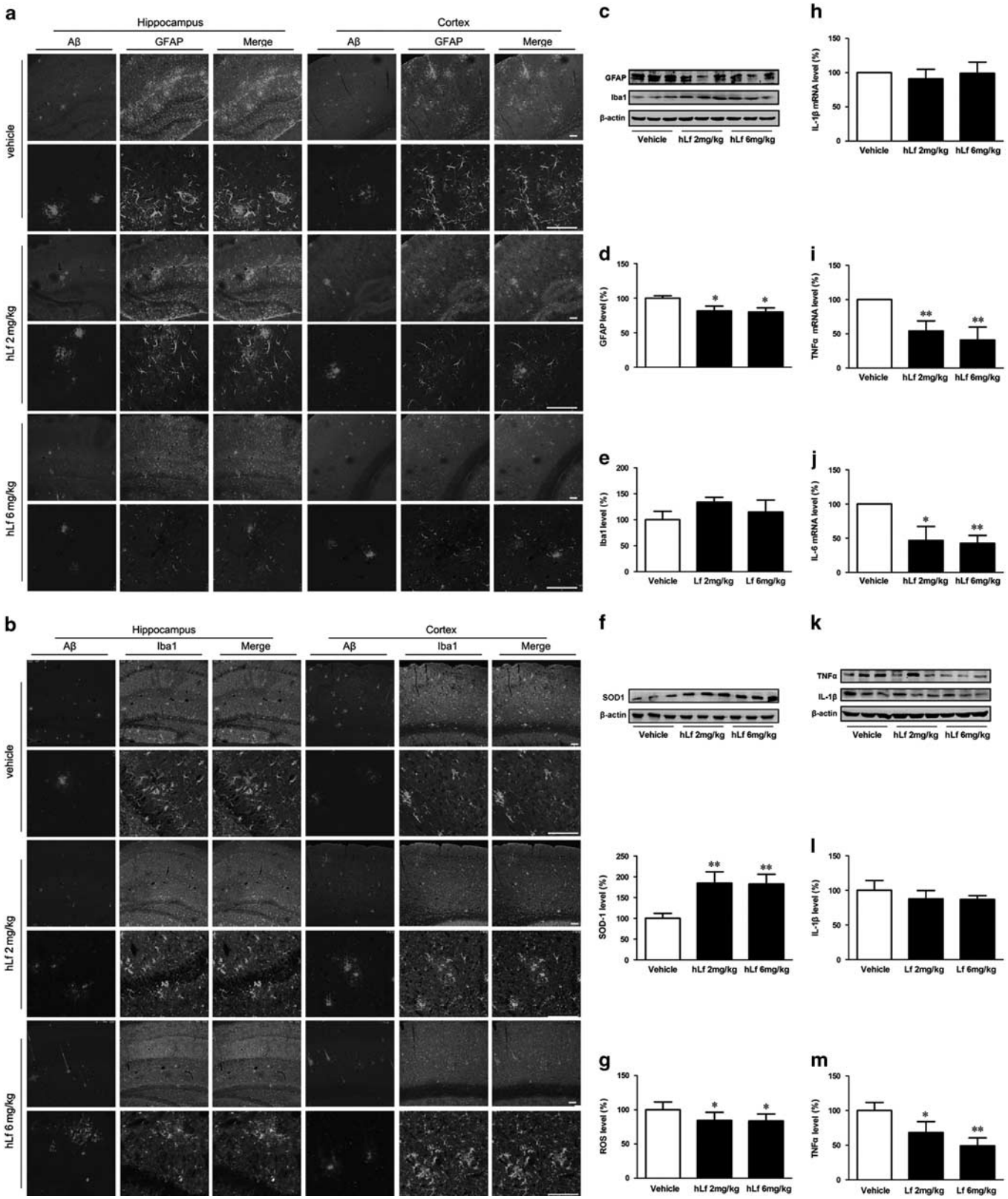

supplemented with a protease inhibitor cocktail (Sigma-Aldrich) and were processed for immunoblot analysis as previously described (Guo *et al*, 2013). The total protein lysate (50 μg) was separated via 10–15% SDS polyacrylamide gels and transferred onto polyvinylidene fluoride (PVDF) sheets (Millipore, Billerica, MA). Primary antibodies against rabbit anti-APP695 (1 : 4000, Chemicon), rabbit anti-APP-CTFs (1 : 4000, Sigma), rabbit anti-ADAM10 (1 : 1000, Millipore), rabbit anti-β-site APP cleavage enzyme 1 (BACE1, 1 : 1000, Sigma), rabbit anti-p-cyclic adenosine monophosphate response element-binding (CREB, 1 : 1000, CST), rabbit anti-CREB (1 : 1000, CST), rabbit anti-p-extracellular-regulated protein kinases (ERK1/2, 1 : 1000, CST), rabbit anti-ERK (1 : 1000, CST), rabbit anti-GFAP (1 : 1000; Santa Cruz Biotechnology), rabbit anti-HIF-1α (1 : 1000, Novus), rabbit anti-Iba1(1 : 1000; Abcam), rabbit anti-IL-1β (1 : 1000, CST), rabbit anti-presenilin 1 (PS1, 1 : 800, Millipore), mouse anti-sAPPα (1 : 500, IBM), mouse anti-sAPPβ (1 : 500, IBM), rabbit anti-superoxide dismutase 1 (SOD1, 1 : 1000, CST), rabbit anti-SYP (1 : 2000; Abcam), rabbit anti-TNFα (1 : 1000; Abcam), rabbit anti-vascular endothelial growth factor (VEGF, 1 : 1000; CST), and mouse anti-β-actin (1 : 10 000, Sigma) were used. Immunoblots were washed and treated with the appropriate species HRP-conjugated secondary antibody (1 : 5000; Santa Cruz Biotechnology), and immunological complexes were visualized by enhanced chemiluminescence (Pierce, Rockford, IL) using a ChemiDoc XRS system and the accompanying Quantity One software (Bio-Rad, Hercules, CA). The immunoreactive bands were quantified using Image-pro Plus 6.0 analysis software.

Real-Time PCR and Assay for ROS Formation

Total RNA was isolated from the cerebral cortex tissues utilizing TRIzol (Invitrogen) according to the manufacturer's instructions. Two micrograms of total RNA from each sample was reverse transcribed using a Prime ScriptTM RT Reagent Kit (Takara, Otsu, Japan). Quantitative PCR assays were performed with SYBR Green PCR Master mix (Promega, Madison, WI, USA) using a MiniOpticon Real-Time PCR detection system (Bio-Rad), and the values were normalized to GAPDH. Each cDNA sample was tested in triplicate. The following PCR primers were used for quantification: TNFα: forward, 5′-AGCCCCCAGTCTGTATCC TT-3′ and reverse, 5′-ACAGTCCAGGTCACTGTCCC-3′; IL-1β: forward, 5′-TTCAAATCTCGCAGCAGCAC-3′ and reverse, 5′-GTGCAGTTGTCTAATGGGAACG-3′; IL-6: forward, 5′-TGTCTATACCACTTCACAAGTCGGAG-3′ and reverse, 5′-GCACAACTCTTTTCTCATTTCCAC-3′; GAPDH: forward, 5′-GGATTTGGTCGTATTGGG-3′ and reverse, 5′-TCGCTCCTGGAAGATGG-3′. ROS levels in the brain tissues homogenates were assessed using 2′,7′-dichlorofluorescein diacetate (DCFH-DA) according to the manufacturer's instructions (Jiancheng Biology, Nanjing, China). DCF fluorescence was detected at 525 nm emission using a microplate reader (Synergy/H1, BioTek).

Statistical Analyses

The results are expressed as the mean ± SEM. Repeated measures analysis of variance (ANOVA) was performed for the Morris water maze tests of the latencies and path lengths; differences among the means were evaluated with multivariable ANOVA. Other comparisons were determined by one-way ANOVA followed by *post hoc* Bonferroni or Tamhane's T2 tests when appropriate. All data were analyzed using SPSS 16.0 software, and differences were assumed to be highly statistically significant if the probability (p) value was <0.01 and statistically significant if $p<0.05$.

RESULTS

Lf Treatment Increases Body Weight Gain and Rescues Cognitive Decline in APP/PS1 Mice

To determine the effects of an intranasal hLf administration in a mouse model of AD, the body weights of the animals and their performance on the MWM tests were evaluated. Following a 3-month treatment regimen with either hLf or vehicle, the body weights of the mice were statistically increased in the hLf-treated group relative to the vehicle controls ($p<0.05$, Figure 1a), suggesting that Lf treatment did not affect the overall health of the animals.

After 90 days of hLf treatment, MWM tests were performed to validate whether Lf treatments affect learning and memory in APP/PS1 mice. The results of the visible platform tests did not differ among the groups, nor did the results of the hidden platform tests on the third and fourth days ($p>0.05$, Figure 1b). However, in the subsequent hidden platform testing, the hLf-treated APP/PS1 mice showed a decrease in escape latency compared with the untreated group from the fifth day to the seventh day of testing ($p<0.05$; Figure 1b). In the probe trial toward the target quadrant on the eighth day, the passing times of the mice in the hLf treatment group were significantly increased compared with the mice in the untreated group ($p<0.01$; Figure 1c). Taken together, these results indicate that the intranasal hLf treatment was able to improve spatial learning impairment in the AD model.

Figure 3 Effects of lactoferrin (Lf) on oxidative stress and inflammatory reaction in the amyloid precursor protein (APP)/presenilin 1 (PS1) mouse brains. Immunofluorescence labeling and confocal microscopy analysis showing the distribution and expression of β-amyloid (Aβ) (green), glial fibrillary acidic protein (GFAP) (a) and Iba1 (b) in the cortex and hippocampus of the APP/PS1 mouse brains. The images are representative of three independent experiments. Scale bar = 100 μm. (c–e) Western blots demonstrating the protein levels of GFAP and Iba1 in the brains of the human Lf (hLf)-, vehicle-treated APP/PS1 mice. (f) hLf treatment markedly enhanced the superoxide dismutase 1 (SOD1) protein levels in the brains of APP/PS1 mice, and (g) the ROS levels were decreased significantly compared with those of the vehicle-treated controls. (h–j) hLf treatment drastically decreased the brain mRNA expression levels of TNFα and IL-6, whereas the level of IL-1β mRNA did not significantly change compared with that of the vehicle-treated APP/PS1 mice. (k–m) Western blots demonstrating the protein levels of IL-1β and TNFα in the brains of the hLf-, vehicle-treated APP/PS1 mice. β-actin was used as an internal control. All values are the means ± SEM ($n=8$). *$p<0.05$, **$p<0.01$ compared with the vehicle group. A full color version of this figure is available at the *Neuropsychopharmacology* journal online.

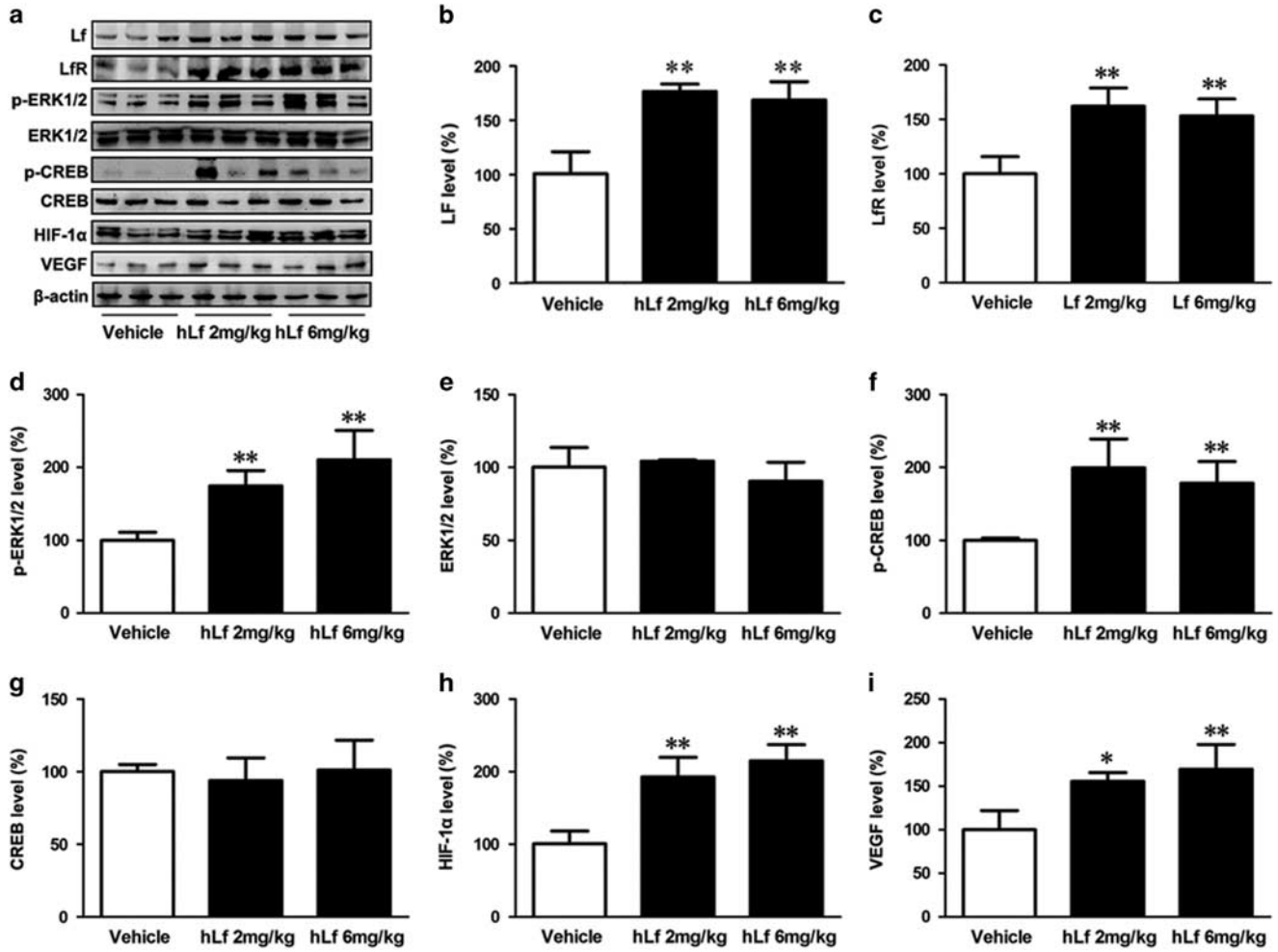

Figure 4 Lactoferrin (Lf) treatment enhanced ERK1/2 phosphorylation and upregulated the activation of CREB and hypoxia-inducible factor 1α (HIF-1α) in amyloid precursor protein (APP)/presenilin 1 (PS1) transgenic (Tg) mouse brains. (a) Change in expression levels of Lf, lactoferrin receptor (LfR), ERK1/2, CREB, HIF-1α, and vascular endothelial growth factor (VEGF) by human Lf (hLf) treatment. β-actin was used as an internal control. (b, c) The treated brain tissues of APP/PS1 mice were assessed for Lf and LfR protein by Western blot analysis. (d–g) The protein levels of total ERK1/2 and CREB were not changed by the different treatments, whereas hLf treatment induced the phosphorylation of ERK1/2 and CREB in the APP/PS1 mouse brains. (h, i) hLf treatment upregulated the expression levels of HIF-1α and VEGF in the APP/PS1 mouse brains. All values are the means ± SEM ($n = 8$). *$p < 0.05$, **$p < 0.01$ compared with the vehicle group.

Lf Treatment Inhibited Aβ Plaque Accumulation by Upregulating ADAM10 and Reduced Synapse Loss in APP/PS1 Mouse Brains

The effects of Lf on Aβ accumulation in APP/PS1 mouse brains were investigated with IHC (Figure 2a). We found that Aβ-immunoreactive plaques were reduced in both the cortex and hippocampus of brains from the hLf-treated group relative to the vehicle controls.

We then assessed the effects of hLf on synapse alterations. As shown in Figure 2c, under hLf treatment, the positive area and the intensity of SYP staining was increased, accompanied by a decreased immunoreactive area of Aβ plaque in the brains of APP/PS1 mice compared with vehicle control mice. In addition, Western blot analysis of the samples using the anti-SYP antibodies confirmed these findings (Figure 2b, $p < 0.01$).

To determine whether the reduction in Aβ generation and aggregation in APP/PS1 mouse brains in the hLf-treated group was correlated with APP processing, we first assessed the expression of APP protein by Western blot. As shown in Figure 2d, we found that compared with the vehicle, treatment with hLf resulted in significantly decreased levels of APP (Figure 2d and e, $p < 0.05$ or $p < 0.01$, respectively). Then, we examined the effect of hLf on the relative APP cleavage enzymes (including ADAM10, BACE1, and PS1) in the APP/PS1 mouse brains. Western blot analysis revealed that hLf treatment significantly increased the levels of ADAM10 and PS1 compared with the vehicle, whereas there were no significant changes in the BACE1 levels in brain tissues between the vehicle control mice and treated mice (Figure 2d, f–h, $p < 0.05$ or $p < 0.01$, respectively). Thus, we further evaluated the effect of hLf on the non-amyloidogenic α-secretase processing of APP in APP/PS1 mice. The results showed that hLf led to a dose-dependent augmentation of sAPPα secretion with a concomitant increase in the

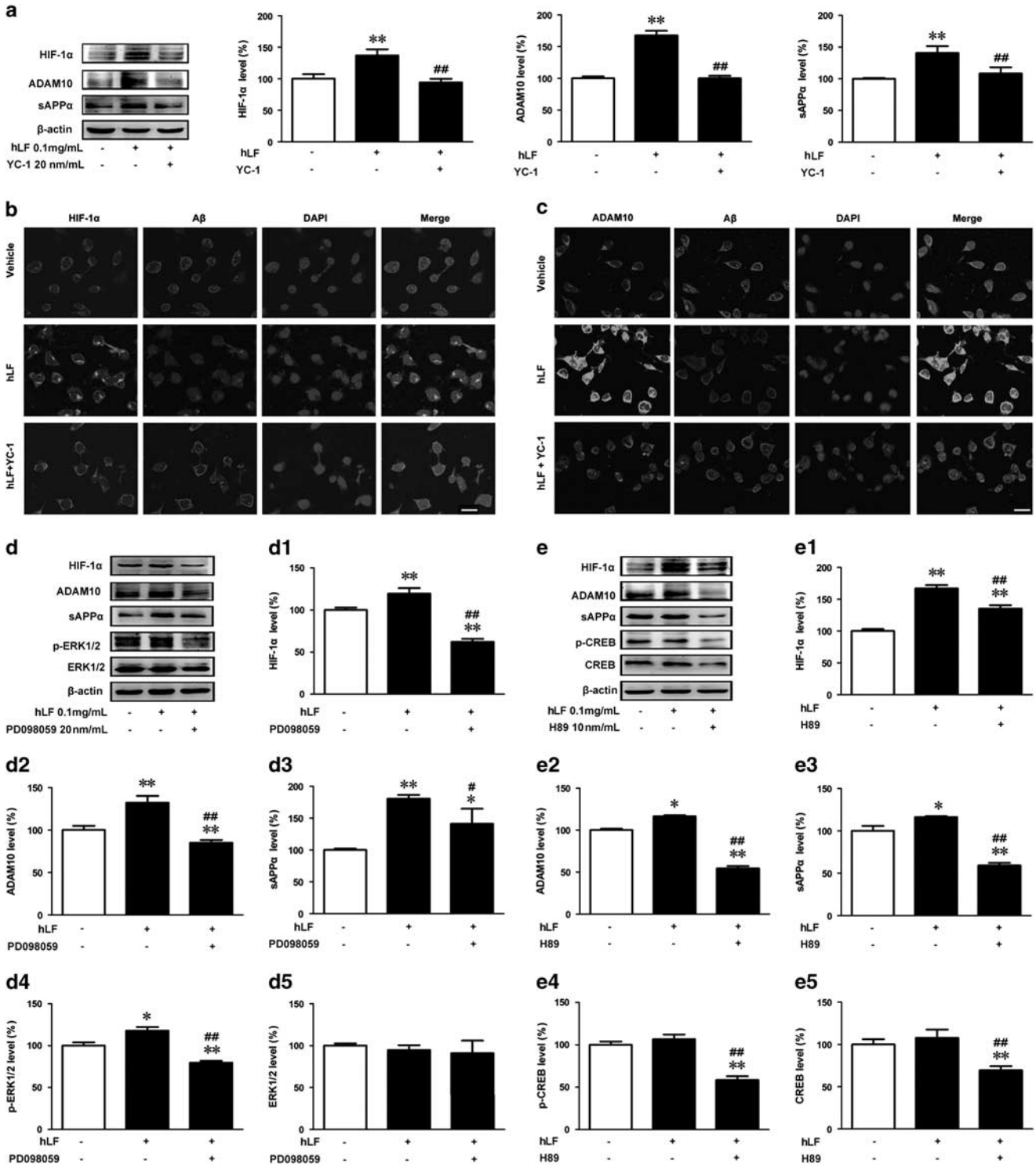

Figure 5 ERK-CREB and hypoxia-inducible factor 1α (HIF-1α) signaling is involved in lactoferrin (Lf)-mediated promotion of amyloid precursor protein (APP) α-proteolysis in N2a cells overexpressing Swedish mutant human APP (APPsw N2a cells). (a) Cultured APPsw N2a cells were treated with human lactoferrin (hLf) in the absence or presence of a HIF-1α selective inhibitor (YC-1) for 24 h. Cell lysates were then prepared from these cells and subjected to Western blot analysis to evaluate APP processing into α-proteolysis using ADAM10, sAPP-α, and HIF-1α antibodies. β-actin was used as an internal control. (b, c) Immunofluorescence labeling using mouse anti-β-amyloid (Aβ) (red) and rabbit anti-HIF-1α/ADAM10 (green) antibodies showed that hLf likely enhanced the expression levels of HIF-1α and ADAM10 and then reduced Aβ generation in APPsw N2a cells. DAPI was used to detect the nuclei (blue). Scale bar = 25 μm. APPsw N2a cells were treated for 24 h with hLf (0.1 mg/ml) in the absence or presence of the ERK1/2 inhibitor PD98059 (d) or the CREB inhibitor H89 (e). The levels of HIF-1α (D1, E1), ADAM10 (D2, E2), sAPPα (D3, E3), phosphorylated ERK1/2 (D4), and CREB (E4) and the total protein levels of ERK1/2(D5) and CREB (E5) were determined by immunoblot analysis. β-actin was used as an internal control. The data represent the means ± SEM of at least three independent experiments; $^{*}p<0.05$, $^{**}p<0.01$ *vs* control group; $^{\#}p<0.05$, $^{\#\#}p<0.01$ *vs* hLf treatment group without YC-1/PD98059/ H89 pretreatment. A full color version of this figure is available at the *Neuropsychopharmacology* journal online.

membrane-bound C-terminal fragment C83 (Figure 2d, i–l, $p<0.05$ or $p<0.01$, respectively).

Therefore, we can infer that Lf promoted non-amyloidogenic processing of APP and endowed it with neurotrophic and neuroprotective properties.

Effects of Lf on Brain Tissue Oxidative Stress and the Inflammatory Signaling Pathway of APP/PS1 Mice

It has been noted in the literature that the AD brain exhibits chronic inflammation primarily around the amyloid plaques of reactive astrocytes and activated microglia (Fuller *et al*, 2010). In the present study, we demonstrated that hLf-treated mice exhibited markedly attenuated GFAP (a marker of astrocytes) immunoreactivities compared to the vehicle-treated mice (Figure 3a, c, and d, $p<0.05$). However, although not reaching statistically significant, we observed a slight increase for the levels of Iba1 in hLf-treated mice compared with vehicle-treated mice (Figure 3b, c, and e, $p>0.05$), suggesting that the progression of the disease might be halted in the early phases, during which time microglia should be beneficial in aiding to clear amyloid and protect neurons (Calsolaro and Edison, 2016).

An important pharmacological approach is supported that may suppress oxidative stress and inflammation, ameliorate cognitive decline, and possibly rescue AD (Daulatzai, 2016). In view of the critical role of oxidative stress in AD-related pathogenesis, we assayed ROS and SOD1 levels in the mouse brains from each experimental group. As shown in Figure 3, in the animals treated with hLf for 90 days, the SOD1 protein levels were markedly increased (Figure 3f, $p<0.01$), whereas the ROS levels were decreased significantly compared with those of the vehicle-treated controls (Figure 3g, $p<0.05$). We then assessed alterations in inflammation-related cytokines in the mouse brain. hLf treatment drastically decreased the brain mRNA expression levels of TNFα and IL-6 by different degrees compared with those of the vehicle-treated APP/PS1 mice (Figure 3i and j, $p<0.05$ or $p<0.01$, respectively), whereas the level of IL-1β mRNA did not significantly change (Figure 3h, $p>0.05$). And the same results for expressed IL-1β (Figure 3k and l, $p>0.05$) and TNFα (Figure 3k and m, $p<0.05$ or $p<0.01$, respectively) were achieved by Western blot.

Collectively, these results suggest that the inhibited inflammatory cascade reaction may correspond to one of the neuroprotective mechanisms of Lf treatment, although the full detailed mechanism has yet to be determined.

Lf Treatment Enhanced ERK1/2 Phosphorylation and Upregulated the Activation of CREB and HIF-1α in APP/PS1 Tg Mouse Brains

To determine whether LfR mediate Lf endocytosis, we investigated the expression of Lf and LfR in APP/PS1 mouse brain. As expected, the protein levels of Lf and LfR were significantly increased in the brain tissues in the Lf treatment condition relative to vehicles (Figure 4a, b, and c, $p<0.01$, respectively), suggesting that LfR is responsive to Lf internalization and therefore mediates the multiple physiological functions of Lf.

Previous studies have indicated that LfR is involved in Lf-induced activation of the ERK1/2 and CREB, these two pathways might regulate each other and co-regulate downstream functions (Ikoma-Seki *et al*, 2015). Moreover, it has been reported that hypoxia contributes to ADAM10 transcription via HIF-1α activation (Barsoum *et al*, 2011), and Lf acts as a normoxic mimetic of hypoxia capable of stabilizing HIF-1α (Zakharova *et al*, 2012). To further investigate the mechanism underlying Lf-mediated upregulation of ADAM10, mitigation of amyloidosis, and inflammation, we next assessed the expression of HIF-1α and VEGF protein, and the activation of ERK1/2 and CREB in the APP/PS1 mouse brains in both hLf- and vehicle-treated mice. As shown in Figure 4, the protein levels of total ERK1/2 and CREB were not changed by the different treatments (Figure 4a, e, and g, $p>0.05$), whereas Lf treatment induced the phosphorylation of ERK1/2 and CREB in the APP/PS1 mouse brains (Figure 4a, d, and f, $p<0.01$). Western blot analysis revealed that hLf treatment also upregulated HIF-1α and VEGF (a downstream target of HIF-1α) (Figure 4a, h, and i, $p<0.05$ or $p<0.01$, respectively). These results demonstrate that Lf concurrently evokes the expressions of ADAM10 and HIF-1α, suggesting that the activation of proteins related to the HIF-1α signaling pathway may be a cue to the neuroprotection of hLf in APP/PS1 Tg mouse brains.

ERK-CREB and HIF-1α Signaling is Involved in Lf-Mediated Promotion of APP α-Proteolysis in APPsw N2a Cells

To test whether the accumulated HIF-1α due to hLf can increase the expression of ADAM10 and sAPPα, we treated APPsw cells with 20 nM YC-1 (an inhibitor for HIF-1α) after 3 h and evaluated the expression at 24 h using Western blot. It was found that incubation of the APPsw cells with YC-1 (20 nM) not only suppressed the hLf-induced accumulation of HIF-1α but also reversed the hLf-dependent increase in ADAM10 and sAPPα synthesis (Figure 5a, $p<0.01$, respectively).

We next explored the effects of hLf on Aβ generation in the APPsw N2a cells to elucidate the downstream factors of HIF-1α using immunofluorescence and confocal microscopy. HIF-1α was weakly expressed in the cytoplasm of vehicle-treated APPsw N2a cells. After the cells were cultured with 0.1 mg/ml hLf for 24 h, the expression of HIF-1α was greatly enhanced and primarily located in the nuclei of the cells, whereas HIF-1α staining was not markedly altered by YC-1 and 0.1 mg/ml hLf co-culture (Figure 5b). Consistent with the above results, double labeling of Aβ and ADAM10 showed that treatment with hLf significantly decreased Aβ immunofluorescence but increased ADAM10 immunoreactive intensity compared with the vehicle. Moreover, these immunoreactivities were significantly inhibited by blocking HIF-1α with YC-1 for 24 h (Figure 5c). Thus, we could reasonably postulate that Lf enhances the α-secretase processing of APP and then reduces Aβ generation via activated HIF-1α.

Next, we sought to further characterize the potential mechanisms underlying the Lf-dependent activation of α-secretase *in vitro*. In light of our *in vivo* studies and previous reports suggesting that the CREB and ERK signaling pathways were activated by Lf (Ikoma-Seki *et al*,

2015) and that the MAPK/ERK pathway is critically involved in HIF-1α-regulated protein synthesis (Guo *et al*, 2016), we evaluated the role of ERK-CREB signaling in HIF-1α-regulated ADAM10 expression. As shown in Figure 5d and e, hLf treatment activated the ERK-CREB pathway, as indicated by the increase in phosphorylated ERK1/2 and CREB. Of utmost interest was the observation that pretreatment of the cultures with a specific ERK or CREB inhibitor, PD98059 (20 μM) or H89 (20 nM), not only blocked ERK1/2 or CREB phosphorylation but also fully prevented HIF-1α-induced ADAM10 and sAPPα increases. Thus, these results suggest that HIF-1α induces the upregulation of ADAM10 via the ERK-CREB pathway.

DISCUSSION

Lf has been implicated in a spectrum of physiopathological events related to iron homeostasis, oxidative defense and inflammation, carcinogenesis, and energy metabolism. Growing evidence suggests the potential use of Lf as a diagnostic marker or as a therapeutic tool (Mayeur *et al*, 2015). Therefore, the use of exogenous Lf as a therapeutic agent will be investigated to identify its roles in AD. Here, we provide the first demonstration that administering 2–6 mg/kg of body weight once a day of hLf for 3 months positively controlled α-secretase ADAM10 expression and markedly reduced the formation of Aβ plaques in the hippocampus of APP/PS1 mice. Moreover, we also found that intranasal administration of hLf enhanced the spatial learning and memory of APP/PS1 mice, with an upregulation of the ERK-CREB and HIF-1α cascade in the brain. These *in vivo* observations were further validated by the administration of hLf and ERK-CREB, and HIF-1α inhibitors in APPsw N2a cells.

Various synthetic and natural products have been investigated as potential alternative therapies for AD. Exogenous Lf has emerged as a very promising anti-inflammatory agent, but less attention has been given to the use of Lf as a neuroprotective factor. Recently, the efficacy of Lf in the treatment of Parkinson's disease has been studied *in vitro*. In the current study, APP/PS1 mice treated intranasally with hLf exhibited increased body weights and better overall health relative to vehicle controls, suggesting that the compound and delivery route were tolerated well by the animals. As expected, we found that exogenous hLf treatment was neuroprotective in APP/PS1 mouse brains, as it reduced the formation of ROS, Iba1, and GFAP immunoreactivity, and the mRNA levels of TNFα and IL-6, and it increased SOD1 activity. However, most importantly, hLf significantly attenuated the formation of Aβ plaques and spatial learning impairment in the APP/PS1 mice. In addition, hLf administration increased the expression level of SYP, which is a synaptic marker involved in disease progression and cognitive decline in AD (Selkoe, 2002). These results suggest that the therapeutic potentials of hLf for mitigating AD-like pathologies deserve further investigation.

In the present study, intranasal Lf treatment significantly decreased the levels of APP695 protein. In concert with reduced Aβ plaques, we also found that hLf increased sAPPα and α-CTF production C83, whereas there were no significant changes in sAPPβ and C99 levels, which indicated that hLf may regulate the metabolism of APP to sAPPα and reduce Aβ levels both *in vitro* and *in vivo*. Our laboratory has previously shown that DFO, an iron chelator, can promote non-amyloidogenic processing of APP through activation of the α-secretase ADAM10, which consequently reduced Aβ generation and improved spatial cognitive learning ability in AD mice (Guo *et al*, 2013). Because Lf has a broad spectrum of biological and pharmacological activities, we then measured the effects of hLf on α-secretase ADAM10, β-secretase BACE1, and γ-secretase PS1. In this study, hLf treatment did not significantly affect BACE1 protein expression. However, hLf administration markedly enhanced the expression level of ADAM10 and PS1 in the APP/PS1 mouse model of AD. These results suggest that hLf is able to mediate APP processing away from the β-secretases and toward the α-secretase pathway as a much-anticipated therapeutic agent in the treatment of neurodegenerative diseases. Indeed, extensive research has focused on the therapeutic application of natural compounds that may increase non-amyloidogenic processing of APP (Shukla *et al*, 2015; Vardy *et al*, 2005; Williams *et al*, 2011).

Direct and/or indirect molecular interactions between Lf and ADAM10 remain to be determined. Previous studies have revealed that synaptic activity induced α-secretase and thereby reduced Aβ generation and release (Kim *et al*, 2010; Wan *et al*, 2012). There is considerable evidence that synaptic numbers and SYP expression may be mediated via the ERK-CREB signaling pathway (Krasnova *et al*, 2013; Liu *et al*, 2016). Moreover, activation of the ERK and CREB signaling may contribute to long-term synaptic plasticity, which is required for memory formation processes, particularly in the hippocampus (Cao *et al*, 2013; Ran *et al*, 2012). How synaptic activity regulates α-secretase remains unclear, although studies implicate HIF-1α as a mediator governing ADAM10 activation (Barsoum *et al*, 2012). Recently, (Shukla *et al* (2015)) observed that ERK phosphorylation upregulated ADAM10 through HIF-1α activation, and Lf is also known as a normoxic mimetic of hypoxia, capable of stabilizing HIF-1α (Zakharova *et al*, 2012). To determine whether upregulation of the ADAM10 protein by hLf in APP/PS1 mice occurred via the same pathway, we analyzed ERK1/2, HIF-1α, and CREB in the extracts of brain tissue. The results showed that hLf treatment in the mice increased the phosphorylation of ERK1/2 and CREB, and upregulated HIF-1α and VEGF. Further, we observed *in vitro* that administration of PD98059 (an inhibitor for ERK), H89 (an inhibitor for CREB), or YC-1 (an inhibitor for HIF-1α) blocked the activation of ADAM10 and the secretion of sAPPα in APPsw cells. Our data are in strong agreement with a previous study that described ERK-mediated activation of ADAM10 through the HIF-1α pathway, suggesting that a component of Lf upregulation of ADAM10 is through activation of HIF-1α (Shukla *et al*, 2015).

The increase in the expression level of Lf and LfR after LF treatment was similar to that reported in ventral mesencephalon neurons (Wang *et al*, 2015). Interestingly, Lf specifically activated the ERK MAPK signaling pathway, which may account for its anti-inflammatory activity (Jiang *et al*, 2011; Yan *et al*, 2013). The neuroprotective effect of exogenous Lf could be explained by the anti-inflammatory properties of Lf (Garcia-Montoya *et al*, 2012; van de Looij

et al, 2014). Indeed, it was shown that hLf can suppress the transcription of TNFα and IL-6 by inhibiting the formation of ROS in our system. Similar effect was observed in immature rat brains with cerebral hypoxia-ischemia (van de Looij *et al*, 2014). Prior studies have documented a significant correlation between Aβ plaque formation, and the activation of microglia and astrocytes in AD brains (Akiyama *et al*, 2000). Although increased positive Iba1 immunoreactivity was not detected as expected, astrocytes significantly expressed less GFAP around Aβ plaques in the brains of the hLf-treated mice, indicating reduced inflammatory reactions due to hLf. On the other hand, as activated microglial cells are believed to be the source of endogenous Lf within the brain (Fillebeen *et al*, 2001), unlessened Iba1 level suggesting that microglia might participate in the effects of exogenous Lf.

In summary, our current study demonstrated that hLf treatment can improve cognitive deficits and Aβ aggregation in APP/PS1 mice after 90 days of administration. Further studies showed that hLf can stimulate ADAM10 activation and promote non-amyloidogenic α-secretase processing of APP by activating the ERK-CREB and HIF-1α signaling pathways in APP/PS1 mice and N2aSW cells. hLf treatment also rescued oxidative stress and neuroinflammation in the brains of APP/PS1 mice. These findings provide mechanistic insight into the potential use of hLf as a therapeutic agent for the treatment of AD.

FUNDING AND DISCLOSURE

The study was supported by the Natural Science Foundation of China (U1608282, 81430025, 31371091), the Basic Scientific Research Fund of Northeastern University (N120820001, N141008001/7, N152006001), the Natural Science Foundation of Liaoning Province (No. 201602249), and the Innovation Team Project of the Department of Education of Liaoning Province (LT2015010). The authors declare no conflict of interest.

REFERENCES

Abbott A (2008). Neuroscience: the plaque plan. *Nature* **456**: 161–164.

Aisen P, Leibman A (1972). Lactoferrin and transferrin: a comparative study. *Biochim Biophys Acta* **257**: 314–323.

Akiyama H, Barger S, Barnum S, Bradt B, Bauer J, Cole GM *et al* (2000). Inflammation and Alzheimer's disease. *Neurobiol Aging* **21**: 383–421.

Arnold RR, Cole MF, McGhee JR (1977). A bactericidal effect for human lactoferrin. *Science* **197**: 263–265.

Barsoum IB, Hamilton TK, Li X, Cotechini T, Miles EA, Siemens DR *et al* (2011). Hypoxia induces escape from innate immunity in cancer cells via increased expression of ADAM10: role of nitric oxide. *Cancer Res* **71**: 7433–7441.

Barsoum IB, Hamilton TK, Li X, Cotechini T, Miles EA, Siemens DR *et al* (2012). Hypoxia induces escape from innate immunity in cancer cells via increased expression of ADAM10: role of nitric oxide. *Cancer Res* **71**: 7433–7441.

Calsolaro V, Edison P (2016). Neuroinflammation in Alzheimer's disease: current evidence and future directions. *Alzheimers Dement* **12**: 719–732.

Cao G, Zhu J, Zhong Q, Shi C, Dang Y, Han W *et al* (2013). Distinct roles of methamphetamine in modulating spatial memory consolidation, retrieval, reconsolidation and the accompanying changes of ERK and CREB activation in hippocampus and prefrontal cortex. *Neuropharmacology* **67**: 144–154.

Crapper McLachlan DR, Dalton AJ, Kruck TP, Bell MY, Smith WL, Kalow W *et al* (1991). Intramuscular desferrioxamine in patients with Alzheimer's disease. *Lancet* **337**: 1304–1308.

Daulatzai MA (2016). Fundamental role of pan-inflammation and oxidative-nitrosative pathways in neuropathogenesis of Alzheimer's disease in focal cerebral ischemic rats. *Am J Neurodegener Dis* **5**: 102–130.

Fillebeen C, Ruchoux MM, Mitchell V, Vincent S, Benaissa M, Pierce A (2001). Lactoferrin is synthesized by activated microglia in the human substantia nigra and its synthesis by the human microglial CHME cell line is upregulated by tumor necrosis factor alpha or 1-methyl-4-phenylpyridinium treatment. *Brain Res Mol Brain Res* **96**: 103–113.

Fuller S, Steele M, Munch G (2010). Activated astroglia during chronic inflammation in Alzheimer's disease–do they neglect their neurosupportive roles? *Mutat Res* **690**: 40–49.

Garcia-Montoya IA, Cendon TS, Arevalo-Gallegos S, Rascon-Cruz Q (2012). Lactoferrin a multiple bioactive protein: an overview. *Biochim Biophys Acta* **1820**: 226–236.

Guo C, Hao LJ, Yang ZH, Chai R, Zhang S, Gu Y *et al* (2016). Deferoxamine-mediated up-regulation of HIF-1alpha prevents dopaminergic neuronal death via the activation of MAPK family proteins in MPTP-treated mice. *Exp Neurol* **280**: 13–23.

Guo C, Wang T, Zheng W, Shan ZY, Teng WP, Wang ZY (2013). Intranasal deferoxamine reverses iron-induced memory deficits and inhibits amyloidogenic APP processing in a transgenic mouse model of Alzheimer's disease. *Neurobiol Aging* **34**: 562–575.

Guo C, Zhang YX, Wang T, Zhong ML, Yang ZH, Hao LJ *et al* (2015). Intranasal deferoxamine attenuates synapse loss via up-regulating the P38/HIF-1alpha pathway on the brain of APP/PS1 transgenic mice. *Front Aging Neurosci* **7**: 104.

Ikoma-Seki K, Nakamura K, Morishita S, Ono T, Sugiyama K, Nishino H *et al* (2015). Role of LRP1 and ERK and cAMP signaling pathways in lactoferrin-induced lipolysis in mature rat adipocytes. *PLoS One* **10**: e0141378.

Iwamaru Y, Shimizu Y, Imamura M, Murayama Y, Endo R, Tagawa Y *et al* (2008). Lactoferrin induces cell surface retention of prion protein and inhibits prion accumulation. *J Neurochem* **107**: 636–646.

Jiang R, Lopez V, Kelleher SL, Lonnerdal B (2011). Apo- and holo-lactoferrin are both internalized by lactoferrin receptor via clathrin-mediated endocytosis but differentially affect ERK-signaling and cell proliferation in Caco-2 cells. *J Cell Physiol* **226**: 3022–3031.

Johnson EE, Wessling-Resnick M (2012). Iron metabolism and the innate immune response to infection. *Microbes Infect* **14**: 207–216.

Kamalinia G, Khodagholi F, Atyabi F, Amini M, Shaerzadeh F, Sharifzadeh M *et al* (2013). Enhanced brain delivery of deferasirox-lactoferrin conjugates for iron chelation therapy in neurodegenerative disorders: *in vitro* and *in vivo* studies. *Mol Pharm* **10**: 4418–4431.

Kawamata T, Tooyama I, Yamada T, Walker DG, McGeer PL (1993). Lactotransferrin immunocytochemistry in Alzheimer and normal human brain. *Am J Pathol* **142**: 1574–1585.

Kim J, Lilliehook C, Dudak A, Prox J, Saftig P, Federoff HJ *et al* (2010). Activity-dependent alpha-cleavage of nectin-1 is mediated by a disintegrin and metalloprotease 10 (ADAM10). *J Biol Chem* **285**: 22919–22926.

Kontoghiorghes GJ, Kolnagou A, Skiada A, Petrikkos G (2010). The role of iron and chelators on infections in iron overload and non iron loaded conditions: prospects for the design of new antimicrobial therapies. *Hemoglobin* **34**: 227–239.

Krasnova IN, Chiflikyan M, Justinova Z, McCoy MT, Ladenheim B, Jayanthi S *et al* (2013). CREB phosphorylation regulates striatal

transcriptional responses in the self-administration model of methamphetamine addiction in the rat. *Neurobiol Dis* **58**: 132–143.

Kruzel ML, Actor JK, Radak Z, Bacsi A, Saavedra-Molina A, Boldogh I (2010). Lactoferrin decreases LPS-induced mitochondrial dysfunction in cultured cells and in animal endotoxemia model. *Innate Immun* **16**: 67–79.

Lammich S, Kojro E, Postina R, Gilbert S, Pfeiffer R, Jasionowski M *et al* (1999). Constitutive and regulated alpha-secretase cleavage of Alzheimer's amyloid precursor protein by a disintegrin metalloprotease. *Proc Natl Acad Sci USA* **96**: 3922–3927.

Leveugle B, Spik G, Perl DP, Bouras C, Fillit HM, Hof PR (1994). The iron-binding protein lactotransferrin is present in pathologic lesions in a variety of neurodegenerative disorders: a comparative immunohistochemical analysis. *Brain Res* **650**: 20–31.

Liu L, Zhu J, Zhou L, Wan L (2016). RACK1 promotes maintenance of morphine-associated memory via activation of an ERK-CREB dependent pathway in hippocampus. *Sci Rep* **6**: 20183.

Mattson MP, Cheng B, Culwell AR, Esch FS, Lieberburg I, Rydel RE (1993). Evidence for excitoprotective and intraneuronal calcium-regulating roles for secreted forms of the beta-amyloid precursor protein. *Neuron* **10**: 243–254.

Mayeur S, Spahis S, Pouliot Y, Levy E (2015). Lactoferrin, a pleiotropic protein in health and disease. *Antioxid Redox Signal* **24**: 813–836.

Orsi N (2004). The antimicrobial activity of lactoferrin: current status and perspectives. *Biometals* **17**: 189–196.

Qian ZM, Wang Q (1998). Expression of iron transport proteins and excessive iron accumulation in the brain in neurodegenerative disorders. *Brain Res Brain Res Rev* **27**: 257–267.

Ran I, Laplante I, Lacaille JC (2012). CREB-dependent transcriptional control and quantal changes in persistent long-term potentiation in hippocampal interneurons. *J Neurosci* **32**: 6335–6350.

Rousseau E, Michel PP, Hirsch EC (2013). The iron-binding protein lactoferrin protects vulnerable dopamine neurons from degeneration by preserving mitochondrial calcium homeostasis. *Mol Pharmacol* **84**: 888–898.

Selkoe DJ (1989). Amyloid beta protein precursor and the pathogenesis of Alzheimer's disease. *Cell* **58**: 611–612.

Selkoe DJ (2002). Alzheimer's disease is a synaptic failure. *Science* **298**: 789–791.

Shukla M, Htoo HH, Wintachai P, Hernandez JF, Dubois C, Postina R *et al* (2015). Melatonin stimulates the nonamyloidogenic processing of betaAPP through the positive transcriptional regulation of ADAM10 and ADAM17. *J Pineal Res* **58**: 151–165.

Takase K (1998). Reactions of denatured proteins with other cellular components to form insoluble aggregates and protection by lactoferrin. *FEBS Lett* **441**: 271–274.

Turner PR, O'Connor K, Tate WP, Abraham WC (2003). Roles of amyloid precursor protein and its fragments in regulating neural activity, plasticity and memory. *Prog Neurobiol* **70**: 1–32.

van de Looij Y, Ginet V, Chatagner A, Toulotte A, Somm E, Huppi PS *et al* (2014). Lactoferrin during lactation protects the immature hypoxic-ischemic rat brain. *Ann Clin Transl Neurol* **1**: 955–967.

Vardy ER, Catto AJ, Hooper NM (2005). Proteolytic mechanisms in amyloid-beta metabolism: therapeutic implications for Alzheimer's disease. *Trends Mol Med* **11**: 464–472.

Velusamy SK, Poojary R, Ardeshna R, Alabdulmohsen W, Fine DH, Velliyagounder K (2014). Protective effects of human lactoferrin during Aggregatibacter actinomycetemcomitans-induced bacteremia in lactoferrin-deficient mice. *Antimicrob Agents Chemother* **58**: 397–404.

Vincent B, Govitrapong P (2011). Activation of the alpha-secretase processing of AbetaPP as a therapeutic approach in Alzheimer's disease. *J Alzheimers Dis* **24**(Suppl 2): 75–94.

Wan XZ, Li B, Li YC, Yang XL, Zhang W, Zhong L *et al* (2012). Activation of NMDA receptors upregulates a disintegrin and metalloproteinase 10 via a Wnt/MAPK signaling pathway. *J Neurosci* **32**: 3910–3916.

Wang J, Bi M, Liu H, Song N, Xie J (2015). The protective effect of lactoferrin on ventral mesencephalon neurons against MPP+ is not connected with its iron binding ability. *Sci Rep* **5**: 10729.

Wang L, Sato H, Zhao S, Tooyama I (2010). Deposition of lactoferrin in fibrillar-type senile plaques in the brains of transgenic mouse models of Alzheimer's disease. *Neurosci Lett* **481**: 164–167.

Williams P, Sorribas A, Howes MJ (2011). Natural products as a source of Alzheimer's drug leads. *Nat Prod Rep* **28**: 48–77.

Yan D, Chen D, Hawse JR, van Wijnen AJ, Im HJ (2013). Bovine lactoferricin induces TIMP-3 via the ERK1/2-Sp1 axis in human articular chondrocytes. *Gene* **517**: 12–18.

Zakharova ET, Kostevich VA, Sokolov AV, Vasilyev VB (2012). Human apo-lactoferrin as a physiological mimetic of hypoxia stabilizes hypoxia-inducible factor-1 alpha. *Biometals* **25**: 1247–1259.